

Optomechanical effects in superfluid properties of BEC in an optical lattice

Research Article

Priyanka Verma¹, Aranya B. Bhattacharjee^{2*}, Man Mohan¹

¹ Department of Physics and Astrophysics, University of Delhi, Delhi-110007, India

² Department of Physics, ARSD College, University of Delhi (South Campus), New Delhi-110021, India

Received 26 April 2012; accepted 5 September 2012

Abstract: We investigate the effects of a movable mirror (cantilever) of an optical cavity on the superfluid properties and the Mott phase boundary of a Bose-Einstein condensate (BEC) in an optical lattice. The Bloch energy, effective mass, Bogoliubov energy and the superfluid fraction are modified due to the mirror motion. The mirror motion is also found to modify the Mott-superfluid phase boundaries. This study reveals that the mirror emerges as a new handle to coherently control the superfluid properties of the BEC.

PACS (2008): 03.75.Kk, 03.75.Lm, 42.50.Lc

Keywords: Bose Einstein condensate • optical cavity • optomechanics
© Versita sp. z o.o.

1. Introduction

Bose-Einstein condensates, which are ensemble of atoms in a single quantum state with long coherence time, offers the possibility to study quantum mechanics in a completely new regime. Ultra-cold atoms in optical lattices exhibit phenomena typical of solid state physics like the formation of Bloch energy bands, tunneling effects and Bloch oscillations. Many of these properties have been subjected to extensive experimental investigations [1].

The fusion of cold atoms and cavity QED (quantum electrodynamics) has made significant experimental progress [2–6]. Theoretically there has been many significant studies on the correlated atom-field dynamics in a cavity. It

has been demonstrated that the strong coupling of the BEC atoms to the optical-cavity mode modifies the resonance frequency of the optical-cavity [7]. Finite cavity response time leads to damping of the coupled atom-field excitations [8]. The driving field in the optical-cavity can substantially increase the localization and the cooling properties of the system [9, 10]. It has been shown that in a cavity the atomic backaction on the field introduces atom-field entanglement which modifies the associated quantum phase transition [11, 12]. The optical field and the condensate atoms are entangled if the atoms are in a superfluid state, in which case the photon statistics typically exhibits complicated multimodal structures [13]. Studies have indicated that the Bloch energy, effective mass, Bogoliubov energy and the superfluid fraction of a condensate are significantly modified if the atoms are enclosed inside an optical cavity [14] and that the light transmitted from the optical cavity can be used as a probe

*E-mail: bhattach@arsd.du.ac.in

to study the superfluid fraction of the BEC [15]. Overlapping stability regions in the quantum phase diagrams have been predicted for a BEC in an optical cavity[16]. Studies on the Dicke model of the BEC in optical cavities show some exotic phase diagrams [17–21].

Recently the field of cavity optomechanics has become an attractive research topic with a wide variety of systems ranging from gravitational wave detectors [22, 23], nanomechanical cantilevers [24–29], vibrating microtoroids [30, 31], membranes [32], Bose-Einstein condensate [33–45] and atomic ensembles [46–51]. A cavity optomechanical system, generally consists of an optical cavity with one movable end mirror. Such a system is utilized to cool a micromechanical resonator to its ground state by the pressure exerted by the cavity light field on the movable mirror. The studies on cavity opto-mechanics of atoms show that sufficiently strong and coherent coupling would enable studies of atom-oscillator entanglement, quantum state transfer, and quantum control of mechanical force sensors. Due to coupling between the condensate wavefunction and the cantilever, mediated by the cavity photons, the cantilever displacement is expected to strongly influence the superfluid properties of the condensate [35]. Coupled dynamics of a movable mirror and atoms trapped in the standing wave light-field of a cavity were studied [51] recently. It was shown that the dipole potential in which the atoms move is modified due to the backaction of the atoms and that the position of the atoms can become bistable. In this paper, we investigate the effects of a movable cavity mirror on the superfluid properties and the Mott-superfluid phase boundary of a BEC confined in an optical cavity.

2. The opto-mechanical Bose-Hubbard Hamiltonian and the effective optical lattice

In the following we will closely follow our earlier works [14, 15, 35, 36] and review some of our earlier results for the sake of continuity. The model studied here consists of an elongated BEC of N two-level ^{87}Rb atoms in the $|F = 1\rangle$ state with mass m and atom transition frequency ω_a of the $|F = 1\rangle \rightarrow |F' = 2\rangle$ transition of D_2 line of the ^{87}Rb atom, interacting with a single standing-wave cavity mode of frequency ω_c . The one dimensional optical lattice potential formed inside the optical cavity is the result of standing wave in the cavity. There is a coupling between the external field incident from one of the side mirrors and the field prevailing inside the cavity. If photon leakage is minimum then the whole system inside the cavity is fully isolated from the environment and it makes the system

coherent. This high-Q optical cavity thus preserves the quantum mechanical nature of the light-field for the entire duration of the experiment. Our model is restricted to a single longitudinal cavity mode by assuming that the longitudinal-mode spacing is much larger than the frequency shift of the cavity due to induced resonance. Also the axial mode frequency is taken to be much smaller than the transverse direction frequency of the harmonic trap so that the transverse degree of freedom is frozen out and the system effectively reduces to a one dimensional elongated BEC. One of the mirrors of the optical cavity is allowed to move with a frequency Ω_m . The frequency of the coherent laser beam is represented by ω_p and its amplitude by η . The strength of the coupling between the movable mirror and the optical mode is denoted by ϵ . Here ϵ is a dimensionless quantity represented by $\epsilon = (x_o/\Omega_m) \frac{d\omega_p}{dx} \Big|_{x=0}$ where x_o is the zero-point motion of the mechanical mode. Here $x_o = \sqrt{\hbar/(2M_{eff}\Omega_m)}$ and M_{eff} is the effective mass of the movable mirror. We begin with an Optomechanical type of Hamiltonian (H_{OM}) for a single particle in rotating wave and dipole approximation as [35]

$$H_{OM} = \frac{P^2}{2m} - \hbar \Delta_a \sigma^+ \sigma^- - \hbar \Delta_c a^\dagger a - i\hbar g(x)(\sigma^+ a - \sigma^- a^\dagger) - i\eta\hbar(a - a^\dagger) + \hbar\Omega_m a_m^\dagger a_m + \hbar\epsilon\Omega_m a^\dagger a (a_m + a_m^\dagger), \quad (1)$$

where $P^2/2m$ is the kinetic energy of the atom, $\hbar\Delta_a \sigma^+ \sigma^-$ is the electronic atomic energy, $\hbar\Delta_c a^\dagger a$ is the energy of the intracavity photons, $i\hbar g(x)(\sigma^+ a - \sigma^- a^\dagger)$ is the space dependent atom-photon interaction energy and $i\eta\hbar(a - a^\dagger)$ is the energy of pump laser. Also $\Delta_a = \omega_p - \omega_a$ and $\Delta_c = \omega_p - \omega_c$ represent the large atom-pump and cavity-pump detuning respectively. Coupling between atom-field is represented by $g(x) = g_o \cos(kx)$ and the symbols σ^+ , σ^- are the usual Pauli matrices. g_o is the amplitude of the atom-photon coupling. The annihilation operator for the mechanical mode is denoted by a_m and a is the annihilation operator for the cavity photon. The excited state can be removed adiabatically from the Heisenberg equation of motion for large detuning Δ_a . Using the Heisenberg equation of motion for the atomic degrees of freedom σ^- and σ^+

$$\begin{aligned} \dot{\sigma}^- &= \frac{i}{\hbar}[H_{OM}, \sigma^-], \\ \dot{\sigma}^+ &= \frac{i}{\hbar}[H_{OM}, \sigma^+], \end{aligned} \quad (2)$$

we get

$$\begin{aligned} \dot{\sigma}^- &= -i \Delta_a \sigma_z \sigma^- + g(x) \sigma_z a, \\ \dot{\sigma}^+ &= i \Delta_a \sigma^+ \sigma_z + g(x) \sigma_z a^\dagger. \end{aligned} \quad (3)$$

Using the condition that $\dot{\sigma}^- = 0$ and $\dot{\sigma}^+ = 0$ in the steady state we get the following expressions for the Pauli matrix operators

$$\begin{aligned}\sigma^- &= \frac{g(x)a}{i\Delta_a}, \\ \sigma^+ &= \frac{-g(x)a^\dagger}{i\Delta_a}.\end{aligned}\quad (4)$$

Substituting Eq. 4 in Eq. 1, we derive an expression for the single-particle hamiltonian as

$$\begin{aligned}H_o &= \frac{P^2}{2m} + \hbar U_o \cos^2(kx)(V_{cl} + a^\dagger a) - i\eta\hbar(a - a^\dagger) \\ &\quad - \hbar\Delta_c a^\dagger a + \hbar\Omega_m a_m^\dagger a_m + \hbar\epsilon\Omega_m a^\dagger a(a_m + a_m^\dagger),\end{aligned}\quad (5)$$

where, $U_o = \frac{g_o^2}{\Delta_a}$ is the height of the optical lattice potential per photon and V_{cl} is the added classical potential. The coupling between the condensate and the cavity gets reduced when $U_o > 0$ as compared to the case $U_o < 0$ because for $U_o > 0$ the lowest bound state is attracted to the nodes of light field. Here we will always take $U_o > 0$. This implies that the cavity optical lattice and the atomic density weakly depend upon each other and the resulting non-linearity is negligible. For $U_o < 0$, the atomic density and the optical lattice depend upon each other and the system becomes highly non-linear [16]. The optical lattice potential is of period $\lambda/2$ and depth $\hbar U_o(V_{cl} + a^\dagger a)$. The Hamiltonian in second quantization can be written as

$$\begin{aligned}H &= \int d^3x \Psi^\dagger(\vec{r}) H_o \Psi(\vec{r}) \\ &\quad + \frac{1}{2} \frac{4\pi a_{sc} \hbar^2}{m} \int d^3x \Psi^\dagger(\vec{r}) \Psi^\dagger(\vec{r}) \Psi(\vec{r}) \Psi(\vec{r}).\end{aligned}\quad (6)$$

The second term in the above is the two-body interaction energy with a_{sc} being the s-wave scattering length. $\Psi(\vec{r})$ represents the field operator of the atoms. To derive an expression for the corresponding Opto-Mechanical Bose Hubbard (OMBH) Hamiltonian we will substitute the atomic field operator as, $\Psi(\vec{r}) = \sum_j b_j w(\vec{r} - \vec{r}_j)$ where $w(\vec{r} - \vec{r}_j)$ is Wannier function. Here b_j represents the annihilation operator for the bosonic atom at the j^{th} site. With this substitution and assuming nearest neighbour approximation we get [35]

$$\begin{aligned}H &= \frac{U}{2} \sum_j b_j^\dagger b_j^\dagger b_j b_j + \sum_j b_j^\dagger b_j (E_o + \hbar U_o (V_{cl} + a^\dagger a) J_o) \\ &\quad + \sum_j (b_{j+1}^\dagger b_j + b_{j+1} b_j^\dagger) (E + \hbar U_o (V_{cl} + a^\dagger a) J) \\ &\quad - i\eta\hbar(a - a^\dagger) - \hbar\Delta_c a^\dagger a + \hbar\Omega_m a_m^\dagger a_m \\ &\quad + \hbar\epsilon\Omega_m a^\dagger a(a_m + a_m^\dagger),\end{aligned}\quad (7)$$

where,

$$\begin{aligned}U &= \frac{4\pi a_{sc} \hbar^2}{m} \int d^3x |w(\vec{r} - \vec{r}_j)|^4, \\ E_o &= \int d^3x w(\vec{r} - \vec{r}_j) \left(-\frac{\hbar^2 \nabla^2}{2m} \right) w(\vec{r} - \vec{r}_j), \\ E &= \int d^3x w(\vec{r} - \vec{r}_j) \left(-\frac{\hbar^2 \nabla^2}{2m} \right) w(\vec{r} - \vec{r}_{j\pm 1}), \\ J_o &= \int d^3x w(\vec{r} - \vec{r}_j) \cos^2(kx) w(\vec{r} - \vec{r}_j), \\ J &= \int d^3x w(\vec{r} - \vec{r}_j) \cos^2(kx) w(\vec{r} - \vec{r}_{j\pm 1}).\end{aligned}\quad (8)$$

On solving the Heisenberg-Langevin equation of motion for a , b_j and a_m we get

$$\begin{aligned}\dot{a}(t) &= -iU_o (J_o \sum_j b_j^\dagger b_j + J \sum_j (b_{j+1}^\dagger b_j + b_{j+1} b_j^\dagger)) a \\ &\quad + i\Delta_c a + \eta - i\Omega_m \epsilon (a_m + a_m^\dagger) a - \gamma_1 a,\end{aligned}\quad (9)$$

$$\begin{aligned}\dot{b}_j(t) &= -\frac{i}{\hbar} U b_j^\dagger b_j b_j - \frac{i}{\hbar} (E_o + \hbar J_o U_o (V_{cl} + a^\dagger a)) b_j \\ &\quad - \frac{i}{\hbar} (E + \hbar J U_o (V_{cl} + a^\dagger a)) (b_{j-1} + b_{j+1}),\end{aligned}\quad (10)$$

$$\dot{a}_m(t) = -i\Omega_m (a_m + \epsilon a^\dagger a) - \gamma_3 a_m, \quad (11)$$

where γ_1, γ_3 are the damping coefficients for the cavity photon operator and the mirror. In all the calculations throughout the paper we will use $E_o = 0$, $J_o = 0$ which means on-site energies are set to zero in comparison to the contribution of tunneling terms U, J. In this regard the optical lattices are advantageous because by tuning the lattice potential, tunneling can be made fast. We assume that γ_1 is the fastest time scale showing that the cavity decay rate is much larger than the oscillation frequency of bound atoms in the optical lattice of the cavity. The condensate is assumed to remain coherent and robust during the duration of the measurement process. $\gamma_3 < \gamma_1$ and measurements are performed after the photons and phonons have attained their steady state values. Typically $\gamma_1 = 2\pi \times 1.0$ MHz and $\gamma_3 = 2\pi \times 1.0$ kHz. The lifetime of the condensate is about 100 ms [34]. In this limit we can put $\dot{a} = 0$ and this yields the photon steady state a_s . Similarly by taking $\dot{a}_m = 0$ we get the steady state mirror displacement $x_{m,s} = a_{m,s} + a_{m,s}^\dagger$ ($a_{m,s}$ is the steady state phonon number). Within the mean-field approximation (for a large number for condensate atoms) and tight binding model, b_j can be replaced by $\phi_j = u_k e^{ikjd - \frac{i}{\hbar} \mu t}$ in form

of Bloch waves. Here μ is the chemical potential of the system with d the distance between any two lattice sites. Also n_o is the atomic number density equal to $\frac{1}{l} \sum_j b_j^\dagger b_j$ and $\sum_j n_o = N$. Here l is the number of lattice sites. For large number of steady state photons, a_s is replaced by the c -number α and we assume that $a_s^\dagger a_s = F = |\alpha|^2$,

$$|\alpha|^2 = \frac{\eta^2}{\gamma_1^2 + \left[\Delta_c + \left(\frac{2\epsilon^2 \Omega_m^3}{\gamma_3^2 + \Omega_m^2} \right) |\alpha|^2 - U_o(J_o N + 2JN \cos(kd)) \right]^2}. \quad (12)$$

On rearranging the above equation we get the following cubic equation

$$A'_1 F^3 + A'_2 F^2 + A'_3 F + A'_4 = 0, \quad (13)$$

where the coefficients are defined as

$$\begin{aligned} A'_1 &= \left(\frac{2\epsilon^2 \Omega_m^3}{\gamma_3^2 + \Omega_m^2} \right)^2, \\ A'_2 &= 2 \left(\frac{2\epsilon^2 \Omega_m^3}{\gamma_3^2 + \Omega_m^2} \right) [\Delta_c - U_o(J_o N + 2JN \cos(kd))], \\ A'_3 &= \gamma_1^2 + [\Delta_c - U_o(J_o N + 2JN \cos(kd))]^2, \\ A'_4 &= -\eta^2. \end{aligned} \quad (14)$$

Now we can numerically solve the Eq. 13, which is simply a cubic equation.

The optical-lattice effective potential which is

$$V_{op} = \hbar U_o (V_{cl} + |\alpha|^2), \quad (15)$$

is plotted as a function of Δ_c in Fig. 1 and as a function of quasi-momentum kd in Fig. 2 (left plot). As ϵ increases, the optical potential shows a tendency to move towards optical bistability regime on the negative Δ_c side for $\epsilon = 0.004$. The optical lattice is always single valued for $\Delta_c > 0$. The maxima of V_{op} are determined by the condition $\Delta_c - U(J_o N + 2JN \cos(kd)) + \frac{2\epsilon^2 \Omega_m^3}{\gamma_3^2 + \Omega_m^2} = 0$. With increasing ϵ , the maxima also shift towards negative Δ_c .

For $\Delta_c > 0$, the lattice effective potential decreases as the coupling ϵ increases. The optical lattice potential is continuously modified as the condensate moves across the Brillouin zone due to the change in the atom-field interaction as shown in the left plot of Fig. 2.

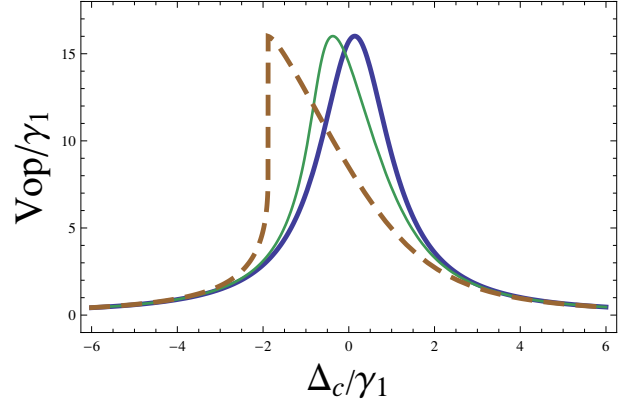


Figure 1. The optical-lattice effective potential modified by the atomic backaction and the mirror motion as a function of the detuning Δ_c/γ_1 for three different values of the mirror-photon coupling, $\epsilon = 0.0$ (thick line), $\epsilon = 0.002$ (thin line) and $\epsilon = 0.004$ (dashed line). The pump amplitude is $\eta/\gamma_1 = 40$, mechanical mirror frequency $\Omega_m/\gamma_1 = 40$, mirror damping $\gamma_3/\gamma_1 = 0.001$, number of particle $N = 100$, $U_o J/\gamma_1 = 0.0007$ and $kd = 0$.

3. Bloch spectrum and effective mass

We will calculate three things in this section the Bloch chemical potential, the lowest Bloch band and the corresponding effective mass assuming the BEC to be in the mean field regime. Substituting the mean field solution for the BEC into Eq. 10, we get

$$\mu = U n_o + (E_o + J_o \hbar U_o [1 + F]) - 2 \cos(kd) J_{eff}, \quad (16)$$

where J_{eff} is defined as a tunneling parameter that depends on k and $|\alpha|^2$, calculated from the cubic equation for F .

$$J_{eff} = -E - \hbar U_o J(1 + F). \quad (17)$$

As the value of mirror-photon coupling (ϵ) increases, the tunneling between the neighboring wells increases since the height of the barriers decreases as is evident from the Fig. 2.

Now to calculate the Bloch energy of the system we use a general expression for the energy per particle as

$$\epsilon(k) = \frac{1}{n_o} \int \mu dn_o, \quad (18)$$

We have plotted the Bloch energy vs kd in the Fig. 3. We have subtracted the ground state energy ($k = 0$) of the system from these curves. A stronger photon-mirror

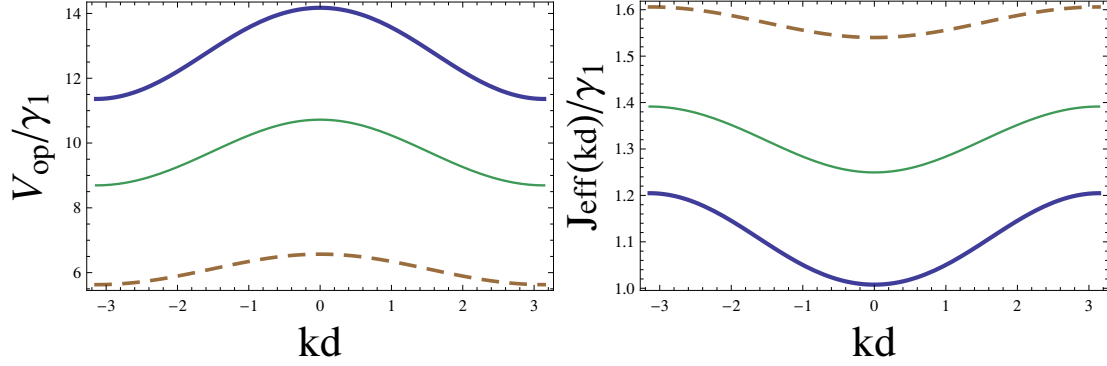


Figure 2. The optical-lattice effective potential (left curve) and the effective tunneling (right curve) as a function of the quasi-momentum kd for three different values of the mirror-photon coupling, $\epsilon = 0.0$ (thick line), $\epsilon = 0.002$ (thin line) and $\epsilon = 0.004$ (dashed line). The pump amplitude is $\eta/\gamma_1 = 40$, mechanical mirror frequency $\Omega_m/\gamma_1 = 40$, mirror damping $\gamma_3/\gamma_1 = 0.001$, number of particle $N = 100$, $U_0J/\gamma_1 = 0.0007$, $E/\gamma_1 = 2.0$ and $\Delta_c/\gamma_1 = 0.5$.

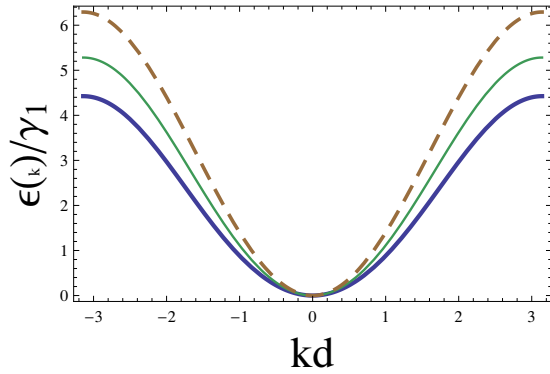


Figure 3. The Bloch spectrum as a function of the quasi-momentum kd for three different values of the mirror-photon coupling, $\epsilon = 0.0$ (thick line), $\epsilon = 0.002$ (thin line) and $\epsilon = 0.004$ (dashed line). The pump amplitude is $\eta/\gamma_1 = 40$, mechanical mirror frequency $\Omega_m/\gamma_1 = 40$, mirror damping $\gamma_3/\gamma_1 = 0.001$, number of particle $N = 100$, $U_0J/\gamma_1 = 0.0007$, $E/\gamma_1 = 2.0$, $U/\gamma_1 = 15$ and $\Delta_c/\gamma_1 = 0.5$. The ground state energy has been subtracted from this plot.

coupling increases the Bloch energy because the corresponding effective optical lattice height decreases. The mirror now emerges as a new tool to coherently manipulate the properties of the BEC.

We will now derive the expression for the effective mass of an atom in the lowest band. The general expression for the effective mass is

$$\frac{1}{m^*} = \frac{1}{\hbar^2} \left. \frac{\partial^2 \epsilon(k)}{\partial k^2} \right|_{k=0}. \quad (19)$$

A plot of the ratio m^*/m of the effective mass to the bare mass as a function of Δ_c , for three different values of ϵ is shown in Fig. 4 (left plot). A peculiar behavior of effective mass becoming less than the bare mass is observed in the

negative detuning side. The maxima in m^* seen in Fig. 4 corresponds to the maxima in V_{op} observed in Fig. 1. The ground state wave function becomes effectively more localized in deeper optical lattices. This results in an increase in the effective mass with a corresponding decrease in the sound velocity. A plot of m^*/m as a function of U_0J/γ_1 is shown in Fig. 4 (right plot). For $U_0J/\gamma_1 \rightarrow 0$ (as the optical lattice vanishes), $m^* \rightarrow m$ as expected. As ϵ increases, the optical lattice barrier height decreases and the tunneling increases accompanied by a decrease in the effective mass as evident from Fig. 4 (right plot).

4. Elementary excitations

The spectrum of elementary excitation is studied in this section. The energy of small perturbations with q as quasi-momentum can be described by the Bogoliubov-spectrum of elementary excitations. We are considering the excitations with respect to the ground state only ($k = 0$). We suppose that μ_0 is the chemical potential for the ground state of translationally invariant lattice. Here $\mu_0 = (\mu)_{k=0}$. We can express μ_0 as

$$\mu_0 = Un_0 - K_{eff}^0 - 2J_{eff}^0, \quad (20)$$

where

$$\begin{aligned} K_{eff}^0 &= -E_0 - \hbar U_0 J_0 [1 + F_0], \\ J_{eff}^0 &= -E - \hbar U_0 J [1 + F_0]. \end{aligned} \quad (21)$$

Here F_0 is the value of F for $k = 0$.

Considering the effect of quantum fluctuations we can replace the annihilation operator b_j by $(\phi_j + \delta_j)e^{-i\mu t/\hbar}$ where

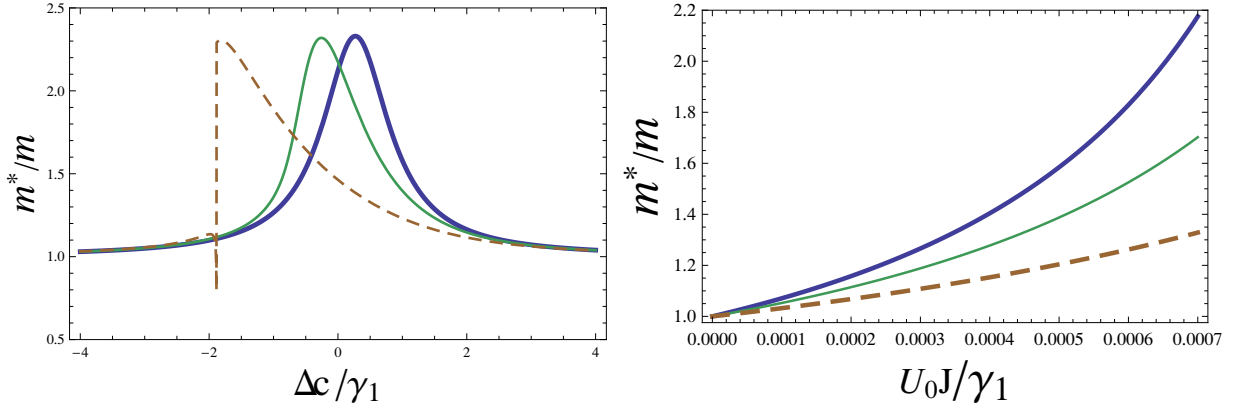


Figure 4. The ratio of effective mass to the bare mass as a function of Δ_c/γ_1 (left plot) and U_0J/γ_1 (right plot) for three different values of the mirror-photon coupling, $\epsilon = 0.0$ (thick line), $\epsilon = 0.002$ (thin line) and $\epsilon = 0.004$ (dashed line). The pump amplitude is $\eta/\gamma_1 = 40$, mechanical mirror frequency $\Omega_m/\gamma_1 = 40$, mirror damping $\gamma_3/\gamma_1 = 0.001$, number of particle $N = 100$, $U_0J/\gamma_1 = 0.0007$, $E/\gamma_1 = 2.0$, $U/\gamma_1 = 15$, $\Delta_c/\gamma_1 = 0.5$ (for right plot) and $kd = 0$.

δ_j is the fluctuation operator. Substituting the above form of annihilation and creation operators in the equation of motion for b_j we get the following equation for δ_j at $k=0$, retaining only terms linear in the fluctuations

$$i \hbar \partial_t \delta_j = (2Un_o - \mu_0) \delta_j + Un_o \delta_j^\dagger - J_{eff}^o (\delta_{j-1} + \delta_{j+1}) - K_{eff}^o \delta_j, \quad (22)$$

which is the Bogoliubov equation for the lattice. Optical lattice potential in the cavity is dependent on the BEC wavefunction hence if there is any variation in the wavefunction it will also affect the optical lattice potential. But the variations we are considering here, are very small therefore we assume that there is no variation in the optical lattice potential due to it. This is true only for $\Delta_c > 0$. Eq. 25 is solved by using the following quasi-particles which diagonalize the Hamiltonian

$$\begin{aligned} \delta_j &= \frac{1}{\sqrt{I}} \sum_q \left[u^q \alpha_q e^{i(qjd - w_q t)} - v_q^* \alpha_q^\dagger e^{-i(qjd - w_q t)} \right], \\ \delta_j^\dagger &= \frac{1}{\sqrt{I}} \sum_q \left[u^{q*} \alpha_q^\dagger e^{-i(qjd - w_q t)} - v_q \alpha_q e^{i(qjd - w_q t)} \right]. \end{aligned} \quad (23)$$

Here u^q and v^q are the Bogoliubov amplitudes. The quasi-particle operators follow Bose-statistics with $[\alpha_q, \alpha_q^\dagger] = \delta_{qq'}$. This yields the Bogoliubov spectrum

$$\begin{aligned} \hbar w_q &= \sqrt{\chi(q) (\chi(q) + 2Un_o)}, \\ \chi(q) &= 4J_{eff}^o \sin^2 \left(\frac{qd}{2} \right). \end{aligned} \quad (24)$$

Imposing the condition that $(u^q)^2 - (v^q)^2 = 1$ we get

$$\begin{aligned} (u^q)^2 &= \frac{\hbar w_q + A}{2\hbar w_q}, \\ (v^q)^2 &= \frac{-\hbar w_q + A}{2\hbar w_q}, \end{aligned} \quad (25)$$

where $A = Un_o + 4J_{eff}^o \sin^2 \left(\frac{qd}{2} \right)$. The influence of ϵ for $\Delta_c > 0$ on the Bogoliubov spectrum is shown in Fig. 5. The mirror-photon coupling is found to enhance the Bogoliubov spectrum which is due to a corresponding decrease in the effective mass. The phononic linear regime is seen to increase for higher ϵ .

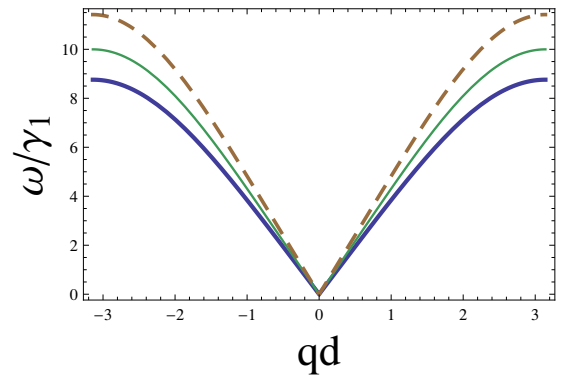


Figure 5. The Bogoliubov spectrum as a function of the quasi-momentum qd for three different values of the mirror-photon coupling, $\epsilon = 0.0$ (thick line), $\epsilon = 0.002$ (thin line) and $\epsilon = 0.004$ (dashed line). The pump amplitude is $\eta/\gamma_1 = 40$, mechanical mirror frequency $\Omega_m/\gamma_1 = 40$, mirror damping $\gamma_3/\gamma_1 = 0.001$, number of particle $N = 100$, $U_0J/\gamma_1 = 0.0007$, $E/\gamma_1 = 2.0$, $U/\gamma_1 = 15$ and $\Delta_c/\gamma_1 = 0.5$.

5. Superfluid fraction

In this section we calculate the superfluid fraction f_s for our system following [52, 53]. An expression for the superfluid fraction can be derived as,

$$f_s = \frac{1}{2N} \sum_{j=1}^l \langle \Psi_o | b_{j+1}^\dagger b_j + b_j^\dagger b_{j+1} | \Psi_o \rangle. \quad (26)$$

Here $|\Psi_o\rangle$ is the ground state of the original Bose Hubbard Hamiltonian and l is the total number of lattice sites. To calculate the f_s we first calculate $\sum_{j=1}^l \langle \Psi_o | b_{j+1}^\dagger b_j + b_j^\dagger b_{j+1} | \Psi_o \rangle$. This yields

$$\begin{aligned} & \sum_{j=1}^l \langle \Psi_o | b_{j+1}^\dagger b_j + b_j^\dagger b_{j+1} | \Psi_o \rangle = \\ & \sum_{j=1}^l \langle \Psi_o | (2|\phi_j|^2 + \delta_{j+1}^\dagger \delta_j + \delta_j^\dagger \delta_{j+1}) | \Psi_o \rangle. \end{aligned} \quad (27)$$

To calculate the above expressions we have used that $\langle \delta \phi \rangle = \langle \Psi_o | \delta \phi | \Psi_o \rangle = 0$, $\phi_{j+1}^\dagger \phi_j = \phi_j \phi_{j+1}^\dagger = \phi_j \phi_j = |\phi_j|^2$. Consequently, we get

$$\begin{aligned} & \langle \Psi_o | (2|\phi_j|^2 + \delta_{j+1}^\dagger \delta_j + \delta_j^\dagger \delta_{j+1}) | \Psi_o \rangle = \\ & x1 + x2 + x3 + x4 + x5, \end{aligned} \quad (28)$$

where

$$\begin{aligned} x1 &= \langle \Psi_o | 2|\phi_j|^2 | \Psi_o \rangle, \\ x2 &= \langle \Psi_o | \frac{1}{l} \sum_q 2 \cos(qd) |u^q|^2 \alpha_q^\dagger \alpha_q | \Psi_o \rangle, \\ x3 &= \langle \Psi_o | \frac{1}{l} \sum_q 2 \cos(qd) |v^q|^2 \alpha_q \alpha_q^\dagger | \Psi_o \rangle, \\ x4 &= \langle \Psi_o | \frac{1}{l} \sum_q (-2v^q u^q \alpha_q \alpha_q) e^{2i(qjd-w_q t)} e^{iqd} | \Psi_o \rangle = 0, \\ x5 &= \langle \Psi_o | \frac{1}{l} \sum_q (-2u^{q*} v^{q*} \alpha_q^\dagger \alpha_q^\dagger) e^{-2i(qjd-w_q t)} e^{-iqd} | \Psi_o \rangle = 0. \end{aligned} \quad (29)$$

On simplifying the above we get following

$$\begin{aligned} & \langle \Psi_o | (2|\phi_j|^2 + \delta_{j+1}^\dagger \delta_j + \delta_j^\dagger \delta_{j+1}) | \Psi_o \rangle = \\ & \langle \Psi_o | 2|\phi_j|^2 | \Psi_o \rangle + \frac{1}{l} \sum_q \langle \Psi_o | (2 \cos(qd) |v^q|^2) | \Psi_o \rangle \\ & + \frac{1}{l} \sum_q \langle \Psi_o | (2 \cos(qd) |v^q|^2 2\alpha_q^\dagger \alpha_q) | \Psi_o \rangle \\ & + \frac{1}{l} \sum_q \langle \Psi_o | (2 \cos(qd) \alpha_q^\dagger \alpha_q) | \Psi_o \rangle \end{aligned} \quad (30)$$

and finally, because $\langle \alpha_q^\dagger \alpha_q \rangle \rightarrow 0$ in the $T \rightarrow 0$ limit, we get

$$\langle \Psi_o | (2|\phi_j|^2 + \delta_{j+1}^\dagger \delta_j + \delta_j^\dagger \delta_{j+1}) | \Psi_o \rangle = 2\phi_j^2 + \frac{1}{l} \sum_q 2 \cos(qd) |v^q|^2. \quad (31)$$

The superfluid fraction at zero temperature is

$$\begin{aligned} f_s &= \frac{1}{2N} \sum_{j=1}^l 2\phi_j^2 + \frac{1}{l} \sum_q 2 \cos(qd) |v^q|^2 \\ &= \frac{l}{N} \left(\phi^2 + \frac{1}{l} \sum_q \cos(qd) |v^q|^2 \right). \end{aligned} \quad (32)$$

The summation is over all quasi-momenta $q = \frac{2\pi}{ld} j$ with $j = 1, \dots, (l-1)$ and ϕ is the value of all ϕ_j in a translationally invariant system. In the limit $d \rightarrow 0$ with q being finite we use the normalization condition as $l\phi^2 + \sum_q |v^q|^2 = N$.

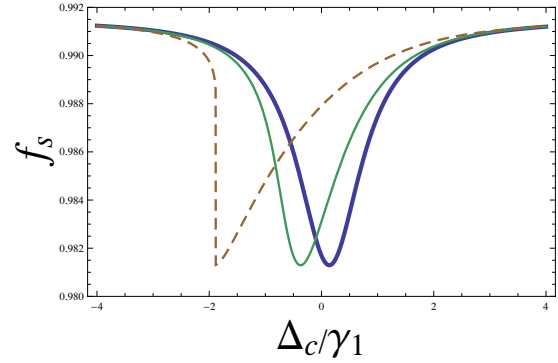


Figure 6. The superfluid fraction as a function of the Δ_c/γ_1 for three different values of the mirror-photon coupling, $\epsilon = 0.0$ (thick line), $\epsilon = 0.002$ (thin line) and $\epsilon = 0.004$ (dashed line). The pump amplitude is $\eta/\gamma_1 = 40$, mechanical mirror frequency $\Omega_m/\gamma_1 = 40$, mirror damping $\gamma_3/\gamma_1 = 0.001$, number of particle $N = 100$, $U_0/\gamma_1 = 0.0007$, $E/\gamma_1 = 2.0$, $U/\gamma_1 = 15$.

A plot of the superfluid fraction as a function of Δ_c is shown in Fig. 6. Just as in the case of effective mass, we observe the onset of multistability in the negative detuning side for $\epsilon = 0.004$. On the positive detuning side, as mirror-photon coupling increases, the superfluid fraction increases since the optical lattice decreases. The moving mirror shakes the optical lattice and transfers the atoms between the wells. This increases the atom number fluctuations. The increase in the superfluid fraction is accompanied by an increase in the atom number fluctuations. This effect can be seen directly by looking at the interference pattern of a BEC released from an optical trap. In contrast to this destructive measurement, one can measure the different phases of the condensate with the mechanical spectrum of the mirror [35].

6. Opto-mechanical effect on the Mott phase

In this section, we now calculate the influence of the mirror motion on the phase diagram of the BEC in the optical cavity. We determine the boundaries of the Mott insulating (MI) states, using the strong-coupling expansion method and closely follow the work of Larson [16]. In the previous sections, the BEC was taken to be in the mean field regime and we assumed that the Wannier functions were independent of the optical lattice. On the contrary in this section, we take into account that the optical lattice potential depends on the atomic density, and hence the Wannier functions depend on the optical lattice. This makes the problem highly nonlinear and the coefficients of Eq. 8 have to be determined self consistently [16]. The optical lattice potential $V = \hbar U_0 a^\dagger a$ neglecting the classical potential. We can expand the steady state (a_s) of a to first order in small tunneling matrix element J and take in the mean field $N = \langle \hat{N} \rangle$.

$$a_s = \frac{\eta}{\gamma_1 - i\Delta'_c} \left\{ 1 - \frac{iU_0 J \hat{B}}{\gamma_1 - i\Delta'_c} \right\}, \quad (33)$$

where $\Delta'_c = \Delta_c - U_0 J_0 N - \epsilon \Omega_m \text{Re}(a_{m,s})$, $\hat{N} = \sum_j b_j^\dagger b_j$ and $\hat{B} = \sum_{ij} b_i^\dagger b_j$. Here $\text{Re}(a_{m,s})$ is the real part of the steady state value of a_m . The steady state value of $a_s^\dagger a_s$ is

$$a_s^\dagger a_s = \frac{\eta^2}{\gamma_1^2 + \Delta_c'^2} \left\{ 1 - \frac{2U_0 J \Delta_c' \hat{B}}{\gamma_1^2 + \Delta_c'^2} \right\}. \quad (34)$$

In the mean field of the steady state photon number $\langle a_s^\dagger a_s \rangle = |\alpha|^2$, the tunneling part of the *OMBH* Hamiltonian is

$$H_{tun} = E + \hbar J U_0 |\alpha|^2 \hat{B}. \quad (35)$$

Now since we are only retaining terms linear in \hat{B} , the effective value of $|\alpha|^2$ is after substituting for $\text{Re}(a_{m,s})$

$$|\alpha|^2 = \frac{\eta^2}{(\Delta_c - U_0 J_0 N \frac{2\epsilon^2 \Omega_m^2}{\gamma_s^2 + \Omega_m^2} |\alpha|^2)^2 + \gamma_1^2}. \quad (36)$$

The rescaled *OMBH* Hamiltonian is obtained as

$$\tilde{H} = -\tilde{t} \hat{B} + \frac{1}{2} \sum_i n_i (n_i - 1) - \tilde{\mu} \hat{N}, \quad (37)$$

where all energy terms are rescaled with respect to U , $\tilde{\mu} = \mu/U$.

$$\tilde{t} = -\frac{E}{U} - \frac{\hbar U_0 J}{U} f(a_s^\dagger a_s), \quad (38)$$

where $f(a_s^\dagger a_s)$ is the value of $a_s^\dagger a_s$ obtained from the cubic equation and depends on the pump intensity. \tilde{t} depends on the atomic density through the Wannier function and at the same time determines the state of the system [16]. We now determine the ground state for a fixed number of particles using the strong coupling expansion technique. The phase boundaries are determined by comparing the energy of the MI state, given by n_0 atoms at each site of the cavity optical lattice, with the corresponding energies of the states with $n_0 + 1$ (particle) atoms or $n_0 - 1$ (holes) particles per site. The nonlinear nature of the problem means that the Wannier functions have to be calculated self consistently [16]. We determine the chemical potential $\tilde{\mu}$ as a function of η for $U_0 > 0$. We have to consider three cases, namely (1)/ $n_0 + 1$, (2)/ n_0 and (3)/ $n_0 - 1$. Here l is the number of lattice sites. The phase diagram is calculated for a fixed number of atoms N and scaling N so as to keep the atomic density constant. The coefficients of Eq. 8 are determined within the Gaussian approximation in which the Wannier functions are replaced by Gaussian functions. The coefficients read as [16]

$$E_0^i = \frac{E_r}{2y_i}, \quad (39)$$

$$J_0^i = \frac{1}{2} [1 - e^{-y_i}], \quad (40)$$

$$E_i = -\frac{[\hbar U_0 f_i(a_s^\dagger a_s)]}{4} e^{-\pi^2/4y_i} (2y_i + \pi^2), \quad (41)$$

$$J_i = \frac{1}{2} e^{-\pi^2/4y_i - y_i}, \quad (42)$$

$$U_i = \frac{4E_r a_{sc}}{\sqrt{2\pi} \Delta_{yz}} y_i, \quad (43)$$

where, $i = 1, 2, 3$ (the three cases mentioned above), $y_i = \sqrt{\frac{E_r}{\hbar U_0 f_i(a_s^\dagger a_s)}}$, Δ_{yz} is the transverse width of the atomic wave packet. E_r is the recoil energy and a_{sc} is the s wave scattering length. The phase diagram in the absence of the mirror motion (Fig. 7a) and with mirror motion (Fig. 7b) clearly shows a reduction in the Mott lobes (indicating an increase in the superfluid phase) in agreement with the previous section. The reduction in the Mott lobe is particularly significant for the $n_0 = 2$ case. The phase diagram without the mirror motion (Fig. 7a), in the $\tilde{\mu} - \eta$ plane shows that the Mott states with higher number of atoms (n_0) have higher energy for large pump strengths, while for moderate pump intensities, states with large n_0 may have smaller energies compared to states with atoms less than n_0 . The mirror motion (Fig. 7b) is seen to increase the energy of the Mott states.

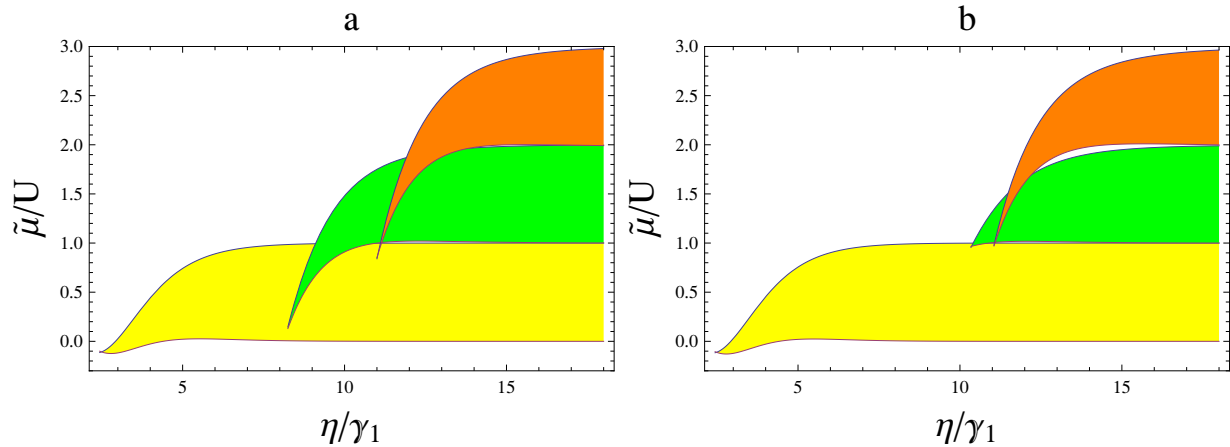


Figure 7. Phase diagram, showing the Mott zones in the scaled chemical potential $\tilde{\mu}/U$ as a function of η/γ_1 for the case without mirror motion (plot (a), $\epsilon = 0$) and with mirror motion (plot (b)), $\epsilon = 0.2$). Here $K = 120$, $\gamma_3 = \gamma_1$, $\Omega_m = 10\gamma_1$ and $\Delta_c = 0.4\gamma_1$. The lowest Mott lobe is for $n_0 = 1$, the next Mott lobe is for $n_0 = 2$ and the top one is for $n_0 = 3$.

7. Conclusions

We have studied the effects of a moving cavity mirror on the Bloch energy, the effective mass, the Bogoliubov excitation, superfluid fraction and the Mott-superfluid phase diagram of a Bose-Einstein condensate confined in an optical cavity. The cavity light field develops a photonic band structure due to the strong coupling with the condensate. Since the moving mirror is coupled to the cavity photons, the photonic band structure is modified due to the mirror motion. For positive detuning case, the mirror motion reduces the optical lattice. The consequence of this effect is to increase the Bloch and the Bogoliubov energies. A decrement in the effective mass of the atoms together with an increment in the superfluid fraction is also observed. The calculated phase diagram also reveals an increment in the superfluid phase due to mirror motion. The mirror appears to be a new handle to coherently control the superfluid properties of the condensate.

Acknowledgements

One of the authors Priyanka Verma thanks the University Grants Commission, New Delhi for the Junior Research Fellowship. A. Bhattacharjee acknowledges financial support from the Department of Science and Technology, New Delhi for financial assistance vide grant SR/S2/LOP-0034/2010.

References

- [1] O. Morsch, M. Oberthaler, *Rev. Mod. Phys.* 78, 179 (2006)
- [2] B. Nagorny, Tn. Elsässer, A. Hemmerich, *Phys. Rev. Lett.* 91, 153003 (2003)
- [3] J. A. Sauer, K. M. Fortier, M. S. Chang, C. D. Hamley, M. S. Chapman, *Phys. Rev. A* 69, 051804(R) (2004)
- [4] A. Öttl, S. Ritter, M. Köhl, T. Esslinger, *Phys. Rev. Lett.* 95, 090404 (2005)
- [5] F. Brennecke, T. Donner, S. Ritter, T. Bourdel, M. Köhl, T. Esslinger, *Nature* 450, 268 (2007)
- [6] Y. Colombe, T. Steinmetz, G. Dubois, F. Linke, D. Hunger, J. Reichel, *Nature* 450, 272 (2007)
- [7] P. Horak, S. M. Barnett, H. Ritsch, *Phys. Rev. A* 61, 033609 (2000)
- [8] P. Horak, H. Ritsch, *Phys. Rev. A* 63, 023603 (2001)
- [9] A. Griessner, D. Jaksch, P. Zoller, *J. Phys. B* 37, 1419 (2004)
- [10] C. Maschler, H. Ritsch, *Opt. Comm.* 243, 145 (2004)
- [11] C. Maschler, H. Ritsch, *Phys. Rev. Lett.* 95, 260401 (2005)
- [12] I. B. Mekhov, C. Maschler, H. Ritsch, *Nature Physics* 3, 319 (2007)
- [13] W. Chen, D. Meiser, P. Meystre, *Phys. Rev. A* 71, 023812 (2007)
- [14] A. Bhattacharjee, *Optics Comm.* 281, 3004 (2008)
- [15] A. Bhattacharjee, T. Kumar, M. Mohan, *Cent. Eur. J. Phys.* 8, 850 (2010)
- [16] J. Larson et al., *New J. Phys.* 10, 045002 (2008)
- [17] G. Chen, X. Wang, J.-Q. Liang, Z.D. Wang, *Phys. Rev. A* 78, 023634 (2008)
- [18] M. J. Bhaseen et. al., *Phys. Rev. A* 85, 013817 (2012)
- [19] M. J. Bhaseen et. al., *Phys. Rev. Lett.* 105, 043001

- (2010)
- [20] Ni. Liu et. al., Phys. Rev. A 78, 023634 (2008)
- [21] Ni. Liu et. al., Phys. Rev. A 83, 033601 (2011)
- [22] T. Corbitt, N. Mavalvala, J. Opt. B: Quantum Semi-class. Opt. 6, S675 (2004)
- [23] T. Corbitt et al., Phys. Rev. Lett. 98, 150802 (2007)
- [24] C. Hühberger-Metzger, K. Karrai, Nature 432, 1002 (2004)
- [25] S. Cigan et al., Nature 444, 67 (2006)
- [26] O. Arcizet et al., Nature 444, 71 (2006)
- [27] D. Kleckner, D. Bouwmeester, Nature 444, 75 (2006)
- [28] I. Favero et al., Appl. Phys. Lett. 90, 104101 (2007)
- [29] C. Regal, J. D. Teufel, K. Lehnert, Nature Physics 4, 555 (2008)
- [30] T. Carmon et al., Phys. Rev. Lett. 94, 223902 (2005)
- [31] A. Schliesser et al., Phys. Rev. Lett. 97, 243905 (2006)
- [32] J. D. Thompson et al., Nature 452, 72 (2008)
- [33] F. Brennecke et al., Science 322, 235 (2008)
- [34] K. W. Murch et al., Nature Physics 4, 561 (2008)
- [35] A. Bhattacharjee, Phys. Rev. A 80, 043607 (2009)
- [36] A. Bhattacharjee, J. Phys. B. 43, 205301 (2010)
- [37] P. Treutlein et al., Phys. Rev. Lett. 99, 140403 (2007)
- [38] G. Szirmai, D. Nagy, P. Domokos, Phys. Rev. A 81, 043639 (2010)
- [39] D. Hunger et al., Phys. Rev. Lett. 104, 143002 (2010)
- [40] B. Chen et al., Phys. Rev. A 83, 055803 (2011)
- [41] G. De. Chiara et al., Phys. Rev. A 83, 052324 (2011)
- [42] S. K. Steinke et al. Phys. Rev. A 84, 023834 (2011)
- [43] D. Hunger et al., Comptes Rendus Physique 12, 871 (2011)
- [44] B. Chen et al., J. Opt. Soc. Am. 28, 2007 (2011)
- [45] K. Zhang et al., Phys. Rev. A 81, 013802 (2010)
- [46] S. Singh, M. Bhattacharya, O. Dutta, P. Meystre, Phys. Rev. Lett. 101, 263603 (2008)
- [47] C. Genes, D. Vitali, P. Tombesi, Phys. Rev. A 77, 050307 (2008)
- [48] H. Ian, Z. R. Gong, Y. Liu, C. P. Sun, F. Nori, Phys. Rev. A 78, 013824 (2008)
- [49] A. A. Geraci, J. Kitching, Phys. Rev. A 80, 032317 (2009)
- [50] K. Hammerer et al., Phys. Rev. Lett. 103, 063005 (2009)
- [51] D. Meiser, P. Meystre, Phys. Rev. A 73, 033417 (2006)
- [52] A. M. Rey et. al., J. Phys. B: At. Mol. Opt. Phys. 36, 825 (2003)
- [53] R. Roth, K. Burnett, Phys. Rev. A 67, 031602 (2003)